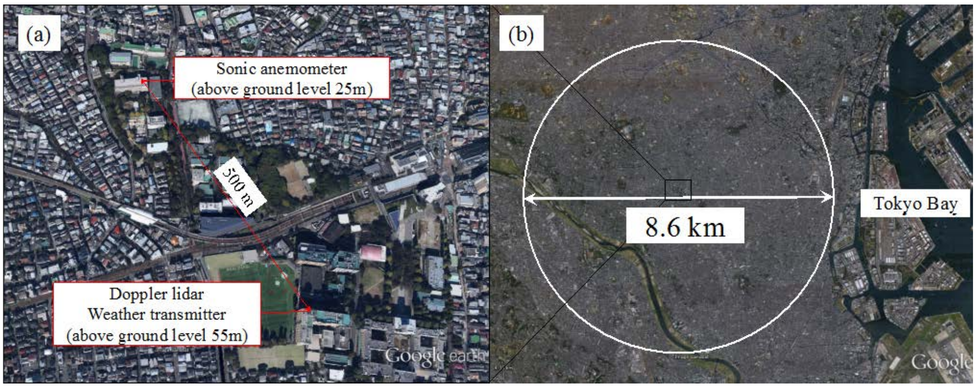

Fig. 1 Deployment of instruments: (**a**) view of the installation site (agl: above ground level), (**b**) area covered by the Doppler lidar.

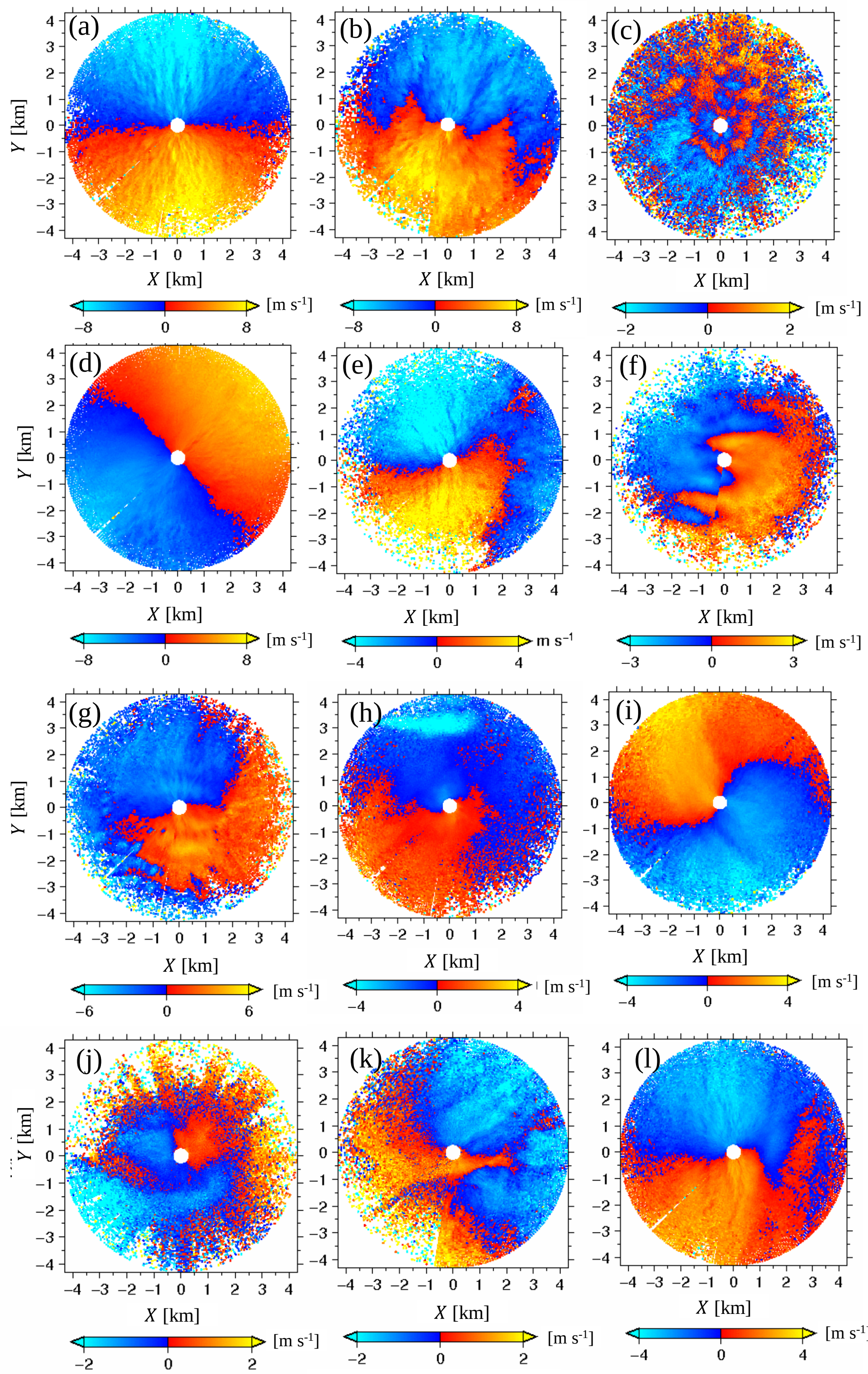

Fig. 2 Horizontal snapshots of the radial velocity measured by the Doppler lidar (DL): (**a**) the category of Streak, (**b**) Mixed, (**c**) Fishnet, (**d**) No streak, (**e**) Front, (**f**) (**g**) (**h**) (**i**) (**j**) (**k**) (**l**)Others. Red (blue) is positive (negative) radial velocity which corresponds to the direction away from (toward) the Doppler lidar.

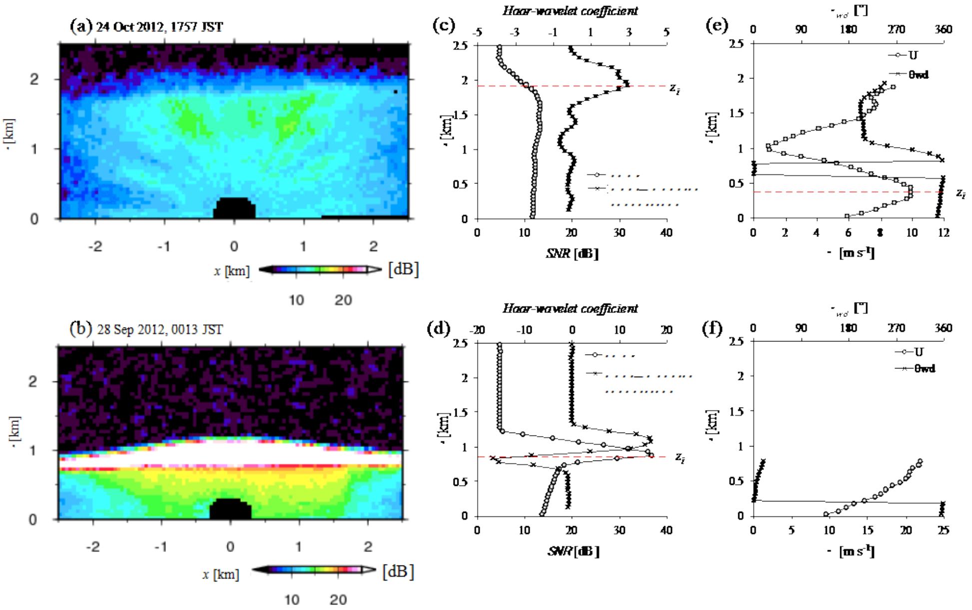

Fig. 3 Vertical snapshots of signal-to-noise ratio (SNR), (**a**) 24 October 2012, 1757 JST, (**d**) 28 September 2012, 0013 JST vertical profiles of averaged SNR for 30 min and its Haar-wavelet coefficient (**b**) 24 October 2012, 1730 to 1800 JST, (**e**) 28 Sep 2012, 0000 to 0030 JST, vertical profiles of horizontal wind velocity and wind direction (**c**) 24 October 2012, 1734 JST, (**f**) 28 September 2012, 0004 JST. The red dotted lines in (**b**), (**c**) and (**e**) show the estimated boundary-layer height for each profile.

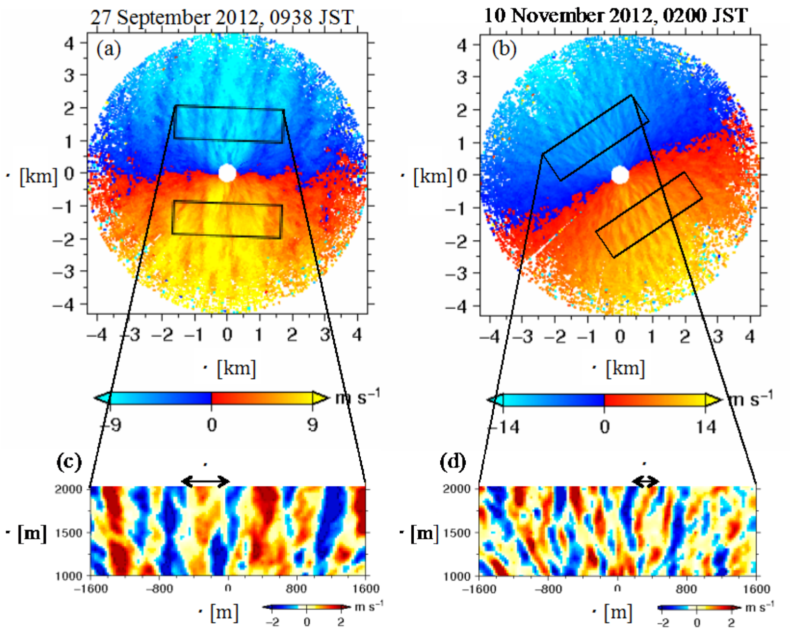

Fig. 4 Horizontal snapshots of radial velocity and streamwise velocity fluctuation, (**a**) (**c**) 27 September 2012, 0938 JST, (**b**) (**d**) 10 November 2012, 0200 JST. The double-headed arrow in (**c**) (**d**) show estimated spacing of streaky structures. The atmospheric parameters of the two cases are as follows; (a) (c) U = 8.4 m s^{-1}, $\Delta U/\Delta z$ = 0.009 s^{-1}, and L = -531 m. (b) (d) U = 10.6, $\Delta U/\Delta z$ = 0.041 s^{-1}, and L = 1136 m.

(a)

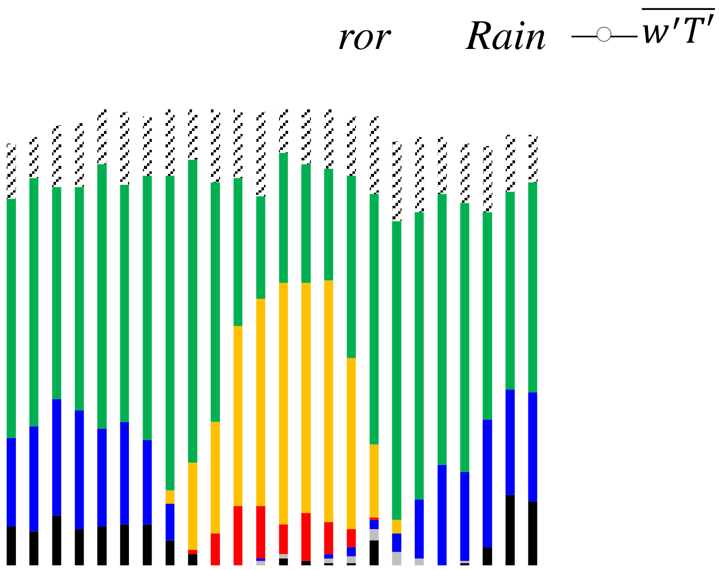

(b)

Fig 5. Diurnal variation in the number of occurrences for each flow pattern, (**a**) autumn, (**b**) winter. One occurrence corresponds to 10 min.

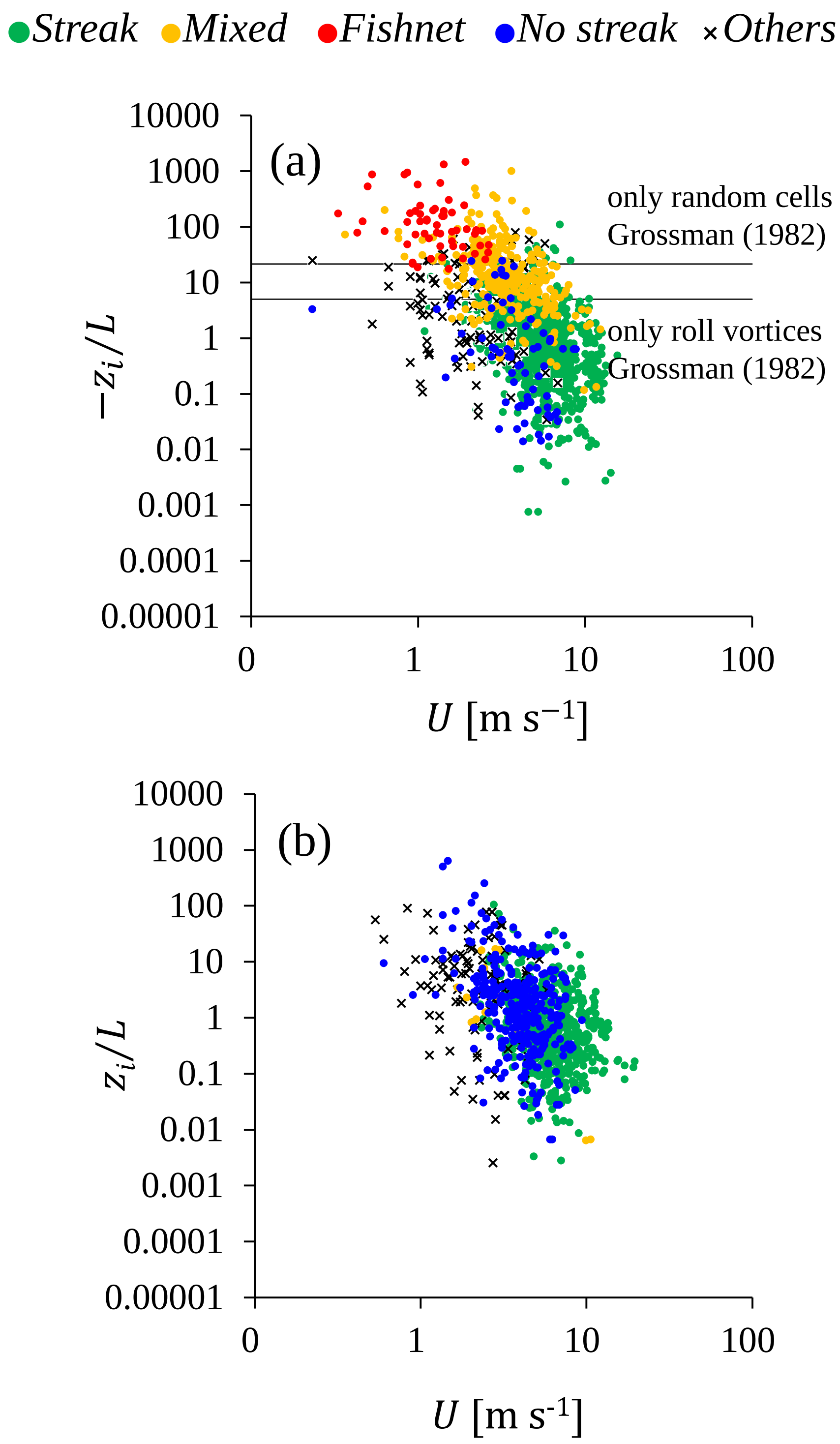

Fig. 6 Stability and horizontal wind speed of each flow pattern, (**a**) unstable ($-z_i/L$ >0), (**b**) stable ($-z_i/L$ <0). The upper line and bottom line in (**a**) are the limit for random cells and roll vortices proposed by Grossman (1982).

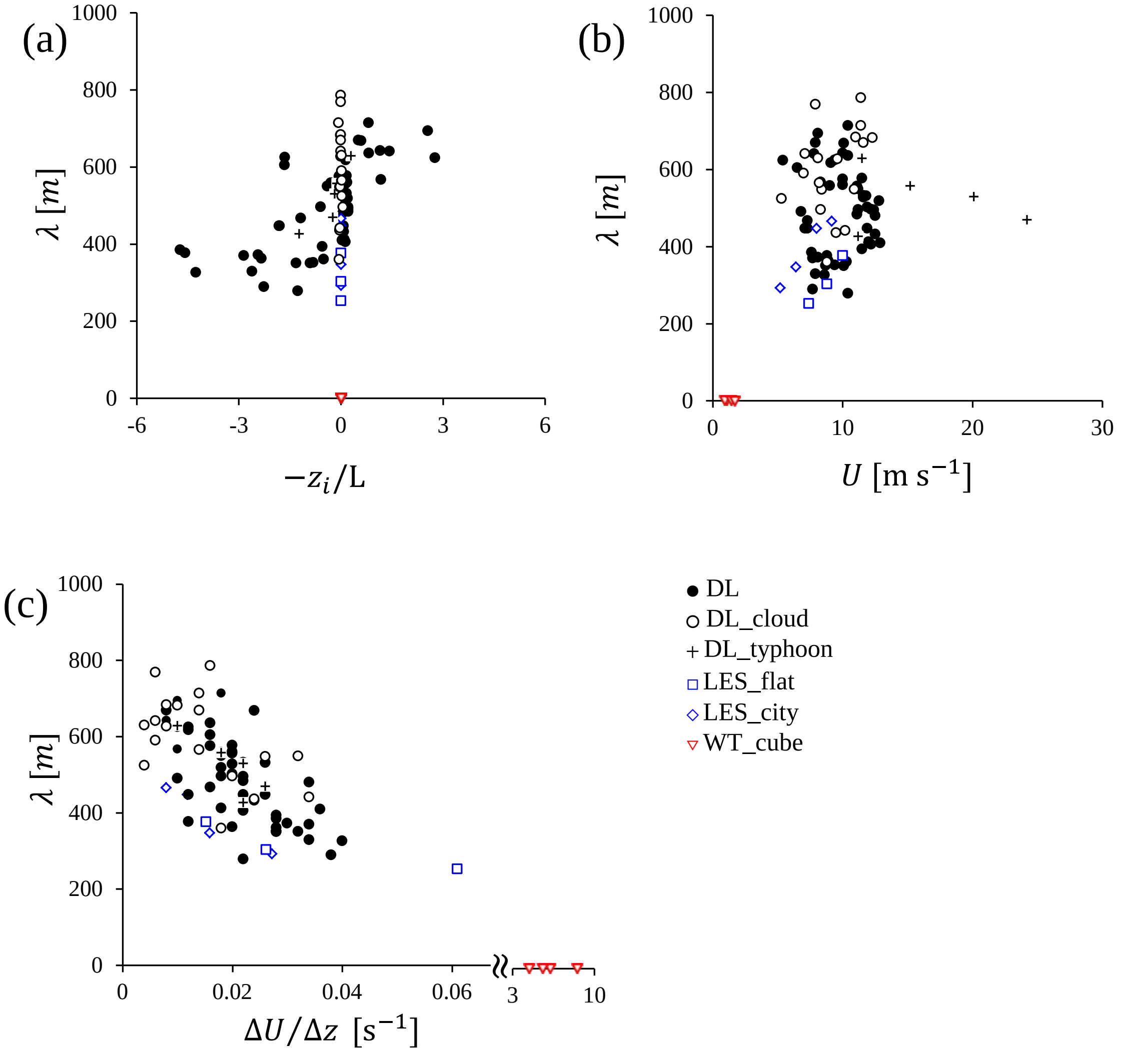

Fig. 7 Relationships between the spacing of streaky structures and meteorological variables: (**a**) stability, (**b**) horizontal wind velocity, and (**c**) wind shear. DL is the Doppler lidar. The symbols are as follows; ● DL, ○ cases of DL with cloud on the top of atmospheric boundary layer, + cases of DL during typhoon. Results of other studies are also shown: □ LES_flat (Lin et al. 1997), ◇ LES_city (Huda et al. 2016), ▽ WT_cube (Takimoto et al. 2013). DL plots include only cases whose mean horizontal wind velocity was greater than 3.5 m s^{-1}. The mean horizontal wind velocity were 30-min average of streamwise wind velocity observed by a sonic anemometer at a height of 25 m above ground level.

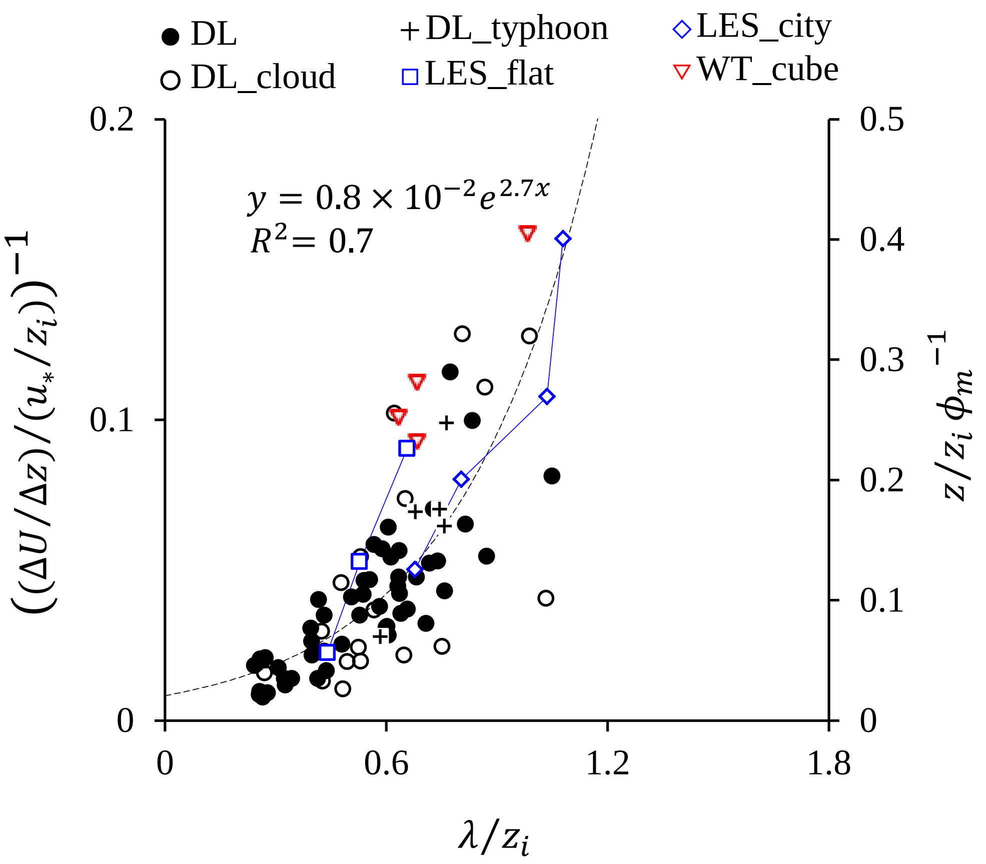

Fig. 8 Relationship between non-dimensional spacing of streaky structures and non-dimensional wind shear. The symbols are same as Fig 7.

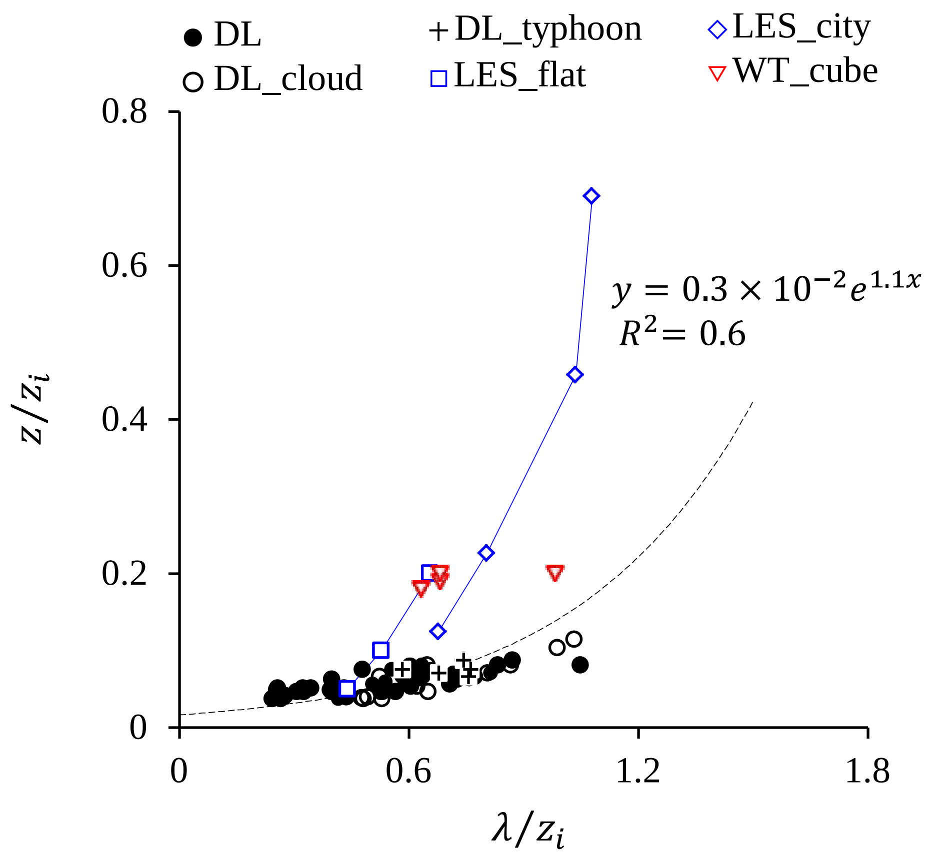

Fig. 9 Relationship between the non-dimensional spacing of streaky structures and non-dimensional height. The symbols are same as Figs 7 and 8.

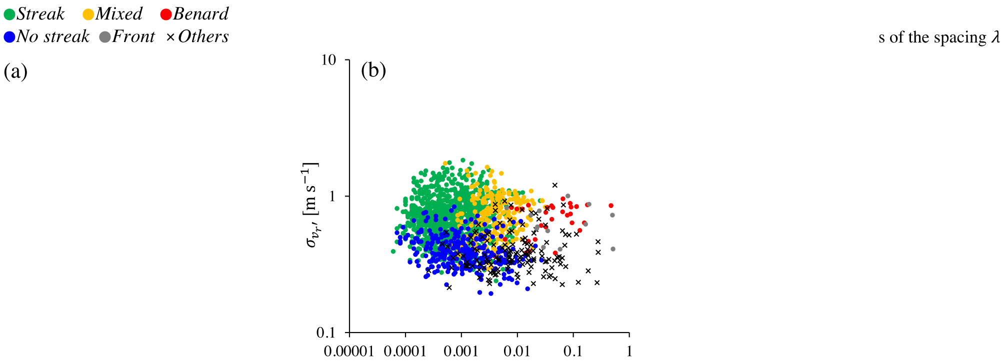

Fig. 10 Statistics of the radial velocity distribution. $cnvergence/U$ is the bulk convergence normalized by the horizontal wind speed, σ_θ is the variance of the wind direction and $\sigma_{v_{r'}}$ is the standard deviation of the fluctuation of radial velocity.

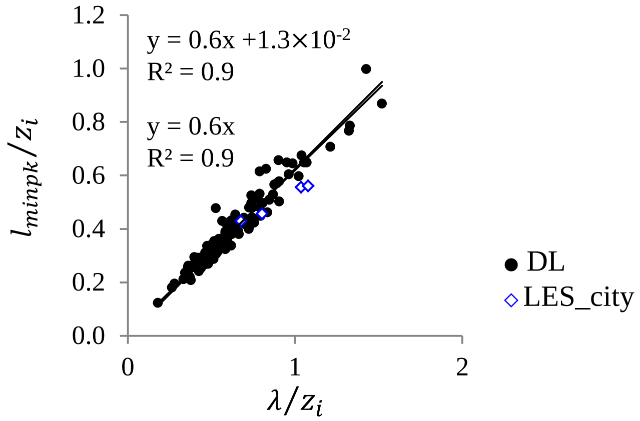

Fig. 11 Relationships between the non-dimensional spacing of streaky structures and the length scales. λ is the spacing of streaky structures, $l_{minpeak}$ is the separation distance from the minimum peak of the two-point correlation, z_i is the boundary layer height, and DL is Doppler lidar. The symbols are as follows: ● DL, ◇ LES_city (Huda et al. 2016).

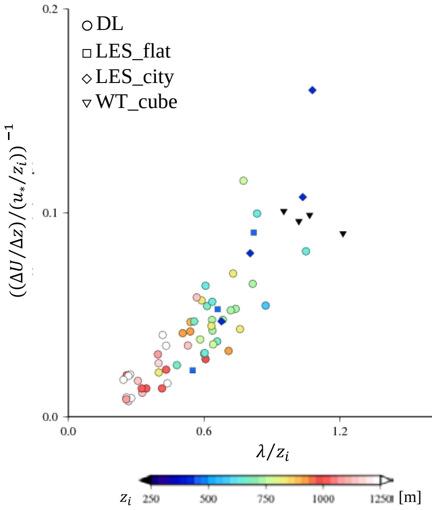

Fig. 12 Relationship between the non-dimensional spacing of streaky structures and non-dimensional wind shear. The colour of plots represents value of z_i. DL is Doppler lidar. The symbols are as follows: ○ DL, □ LES_flat (Lin et al. 1997), ◇ LES_city (Huda et al. 2016), ▽ WT_cube (Takimoto et al. 2013). DL plots include only cases whose mean horizontal wind velocity was greater than 3.5 m s^{-1}. The mean horizontal wind velocity were 30-min average of streamwise wind velocity observed by a sonic anemometer at 25 m above ground level.

Table 1 Thirty-min scan sequence of the Doppler Lidar (DL). PPI is the Plan Position Indicator, RHI is the Range Height Indicator. Azimuths of 0 °, 90 °, 180 ° and 270 ° correspond to the north, east, south, and west directions, respectively.

No	scan mode	number of scan	elevation [°]	azimuth [°]	time [min]
1	PPI	2	0	0~360	4
2	RHI	2	-1~181	135	2.3
3	RHI	2	-1~181	45	2.3
4	PPI	2	0	0~360	4
5	RHI	2	-1~181	135	3
6	PPI	2	0	0~360	4
7	RHI	2	-1~181	135	3
8	PPI	1	0	0~360	3
9	RHI	1	-1~181	135	2.6
total time					28.2

Table 2 Criteria of visual classification

Streak	Clear streaky patterns are seen along the dominant wind direction. The boundary of positive and negative radial velocity is almost straight.
Mixed	Streaky patterns are seen along the dominant wind direction. The boundary of positive and negative radial velocity is distorted.
Fishnet	The boundaries of positive and negative radial velocity have a periodic cell-like (fishnet) pattern.
No streak	Neither streaky nor cell-like patterns is seen. The boundary of positive and negative radial velocity is straight.
Front	Clear convergence line is seen.
Others	Exception to the above five groups above.

Table 3 Other studies cited in Figure 7-9

reference	approach	methodology to estimate length scale	stability	surface	z [m]
Lin et al. (1997)	LES	length scale determined by at the minimum peak of two-point correlation	neutral	flat surface	23, 46, 92
Huda et al. (2016)	LES	wavelength at the peak of the power spectrum density (the dataset was given to us personally and the spacing λ was calculated in the same way as in this paper)	neutral	urban geometry	54, 98, 198, 298
Takimoto et al. (2013)	wind tunnel	length scale determined by at the minimum peak of two-point correlation	neutral	a square array	0.063
				height varying elements	0.061
				two-dimensional street canyon	0.056
				flat surface	0.036